Hyperstar Polyester-Based Functional Nanotheranostics for the Targeted Drug Delivery and Treatment of Cancer

Riyadh Alnasser, Zachary Shaw, and Santimukul Santra*[a]

Abstract: In this study, we have synthesized new class of hyperstar polyester (HSPE) polymer using a functional A_2B monomer and bio-based sorbitol. We hypothesize that by incorporating sorbitol, its amphiphilic nature will give the polymer greater solubility and allow for the encapsulation of wide range of anti-cancer therapeutics. We used potassium methoxide to catalyze the melt polymerization reaction. Using the solvent diffusion method, this polymer was used to construct polymeric nanoparticles to encapsulate therapeutics, in one step, for monitoring drug delivery and treatment.

The cytotoxicity of our HSPE nanoparticles was evaluated by a cell-based MTT assays using prostate cancer cells (LNCaP) and healthy cells (CHO). In addition, the level of internalization of our HSPE nanoparticles was evaluated using fluorescence microscopy. Results showed the HSPE nanoparticles have the capability to target and concurrently image and kill cancer cells. Taken together, these studies indicate the successful development of a new drug delivery system and demonstrated its potential use in the pharmaceutical industry and the field of medicine.

Introduction

The development of new biocompatible polymers is an important research area in the field of medicine. New biomaterials give rise to new diagnostic and therapeutic techniques for many biomedical applications including but not limited to the targeted delivery of cancer therapeutics.[1,2] Biodegradable polymers are macromolecules with backbones that can be degraded easily, in-vivo to nontoxic byproducts.[3–6] Aliphatic polyester polymers are heavily studied because they can be synthesized easily with high molecular weight and high solubility.[7–9] They are divided into two groups according to their origin: natural polymers (from renewable sources), and synthetic polymers (from non-renewable sources), and further classified as linear or branched polymers.[10] Polylactic acid (PLA) and polyacrylic acid (PAA) are the simplest linear polyesters and have been used to formulate nanotherapeutic delivery systems alone or in combination with other polymers. As a derivative of lactic acid, PLA is considered nontoxic due to its natural breakdown to sugar inside the body. However, linear polymers are limited in their use as drug delivery systems due to their high polydispersity, low encapsulation efficiencies, and coil-like morphology with low surface functionality. Thus, branched polymers are a more favored architecture for drug delivery.[11–13]

Branched polymers describe a broad category of polymers including polymeric micelles, dendritic polymers, and hyperbranched polymers, which offer enhanced properties over linear polymers. Polymeric micelles have advantageous properties including a tunable core-shell structure from an assembly of amphiphilic block copolymers, good water solubility due to its amphiphilic shell, and high therapeutic loading capacity of drugs and dyes attributing to its hydrophobic core.[14,15] Dendrimers have unique architectural characteristics including a central core, perfect branching, functional terminal groups, and are monodisperse.[16,17] However, their preparation is tedious and very expensive compared to hyperbranched polymers. Hyperbranched polymers are synthesized easily in a single-step (condensation or ring-opening polymerization methods), are low-cost, and have similar properties as dendrimers for applications in drug delivery including effective cargo-holding polymeric cavities, a higher number of functional end groups, and possess a characteristic three-dimensional structure.[18,19] In addition to their biodegradability and stability, these architectural properties make hyperbranched polyesters a high research interest.[20]

Dr. Santra synthesized a biodegradable hyperbranched polyester (HBPE) suitable for formulating nanoparticles with amphiphilic cavities and hydrophilic terminal groups.[21] In this work, a designer A_2B type monomer was synthesized and polymerized via condensation reactions of the carboxylic acids to the hydroxyl giving a spherical hyperbranched polyester polymer. This polymer was used to formulate Taxol-encapsulating polymeric nanomedicine for targeting lung cancer. Dr. Chow synthesized hyperbranched polyesters fitting to formulate nanoparticles. By reacting an AB monomer with a CD_n monomer via Michael addition, he generated AD_n-type intermediates that through self-condensation yielded a hyperbranched polyester.[19] Dr. Smith used a trifunctional bio-alcohol and a difunctional bio-acid ($A_2 + B_3$ system) to generate a biodegradable HBPE for the controlled time release of small molecule therapeutics.[22] Also utilizing an $A_2 + B_3$ system, Dr. Bruchmann obtained a HBPE via a one-step polycondensation, generating polymers with a high degree of functionality and high molecular weights.[23] This biodegradable polymer would be an ideal material for use in drug delivery systems. Dr. Zabihi

[a] R. Alnasser, Z. Shaw, Dr. S. Santra
Department of Chemistry
Pittsburg State University
1701 S Broadway Street, Pittsburg, KS 66762 (USA)
E-mail: ssantra@pittstate.edu
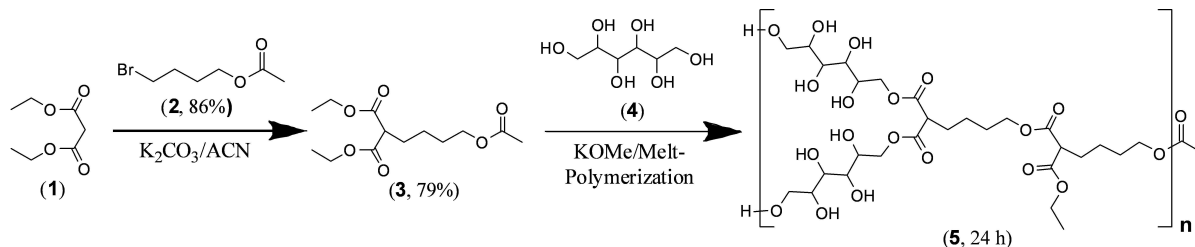
Scheme 1. Synthesis of a new hyperstar polyester (HSPE) polymer using the A₂B monomer derived from diethyl malonate and sorbitol.

synthesized a hyperbranched polyester from step-growth polycondensation reactions between citric acid and glycerol (A_3B+B_3 system). The resulting polymers were loaded with cisplatin (an anticancer drug) and administered to tumor cell line C26, which resulted in 60% cell death after a 72 h incubation period via MTT assay. This assay proved the efficacy of these HBPE polymers as biocompatible therapeutic delivery vehicles for the treatment of cancer.[24–26]

In this direction, we demonstrate the synthesis of biodegradable hyperstar polyester (HSPE) polymer utilizing an A_2B+B_2 system suitable for biomedical applications, particularly for the production of nanoparticles for use as a drug delivery system (Scheme 1). In the synthesis of hyperbranched polymers, the use of A_2B+B_2 binary monomer systems bring lower steric crowding in polymer growth and flexibility in the polymer backbone. This results in higher molecular weight polymers compared to the probability of obtaining low molecular weight crosslinked polymers using other monomer systems. Herein, we obtained our HSPE polymer by an easy, one-step polycondensation reaction in the melt condition. This HSPE polymer is amphiphilic in nature and had improved solubility in organic solvents ($CHCl_3$, DMF, and DMSO) over our previously reported[25] first-generation HBPE polymer (DMF, and DMSO), derived directly from A_2B monomer (**3**, Scheme 1). The functional hydroxyl surface groups can be tailored to facilitate the specific targeting of cancer cell surface proteins, and the ester backbone and high molecular weight provide an excellent capability for biodegradation and the encapsulation of therapeutic cargo. These characteristics would make our newly designed HSPE polymer an ideal candidate to be used as a drug delivery system to treat cancer.

Results and Discussion

Aliphatic hyperbranched polyester polymers have shown moderate drug delivery properties, as reported,[21] due to the hydrophobicity of the polymer backbone. To enhance this property, herein we have designed an amphiphilic HBPE polymer by incorporating hydrophilic sorbitol in the polymer backbone. The addition of sorbitol would facilitate the encapsulation and delivery of wide spectrum of drugs. We demonstrate the synthesis of this novel branched polymer, named hyperstar polyester (HSPE) polymer in Scheme 1. The starting material, 4-bromobutyl acetate (**2**), is synthesized as

previously reported[21,25] and characterized by NMR and FT-IR spectroscopic methods (SI, Figure S1, Figure S2A). The desired monomer structure was formed through selective mono-C-alkylation of diethyl malonate (**1**) with 4-bromobutyl acetate (**2**) in the presence of a weak base in a polar aprotic solvent. The branched functional A_2B monomer (**3**) was purified by column chromatography and then characterized by NMR and FT-IR spectroscopic methods (Figure 1; SI, Figure S2B). Sorbitol (**4**) (a B_2 monomer), was selected as the hydrophilic component to give our proposed HSPE polymer amphiphilicity. The functional A_2B monomer (**3**) copolymerized with sorbitol (**4**), to generate the proposed HSPE polymer through trans-esterification with KOMe as a catalyst, using the melt-polymerization technique. The polymerization reaction was carried out at 140 °C under high vacuum, and polymer samples were periodically taken to determine the reaction progression. We observed that after 24 h, a polymer of desired molecular weight was obtained, which was suitable for formulating drug delivery systems. The resulting polymer samples were purified via a mixed solvent (DMF/Acetone) precipitation method and characterized by NMR and FT-IR spectroscopic methods (Figures 1–3A; SI, Figure S2C).

The ¹H NMR, ¹³C NMR, and FT-IR spectra confirm the presence of carbonyl groups, hydroxyl groups, and ester linkages (Figures 1–3A). As seen in the ¹H NMR (Figure 1) spectrum, the presence of a triplet at 3.4 ppm confirmed the successful synthesis of the A_2B monomer (**3**). The presence of broad peaks at the expected chemical shifts confirmed the formation of a high molecular weight polymer, as demonstrated in Figure 1. We further characterized of both the monomers and polymer by performing ¹³C NMR, as shown in Figure 2. The peaks from 20–30 ppm and 60–80 ppm confirm the incorporation of sorbitol with the A_2B monomer. The presence of ester carbonyl groups at 1720 cm⁻¹ and the presence of hydroxyl groups at 3380 cm⁻¹ in the FT-IR further confirm the successful incorporation of sorbitol into the polyester backbone. Thermogravimetric analysis (TGA) showed moderate thermal stability with 10% weight loss at 265 °C under a nitrogen atmosphere, which is a desired requirement for biostability, as our polymer will need to be stable at biological temperatures (37 °C) (Figure 3B).[27,28] The formation of a high molecular weight polymer was confirmed by performing MALDI-TOF mass spectroscopy (Figure 4A). As indicated, we have achieved a high molecular weight polymer ($M_n = 37\ 615$). To monitor polymerization and calculate the average molecular weight (M_w) of the HSPE polymer, samples were characterized by Gel Permeation Chromatography (GPC)
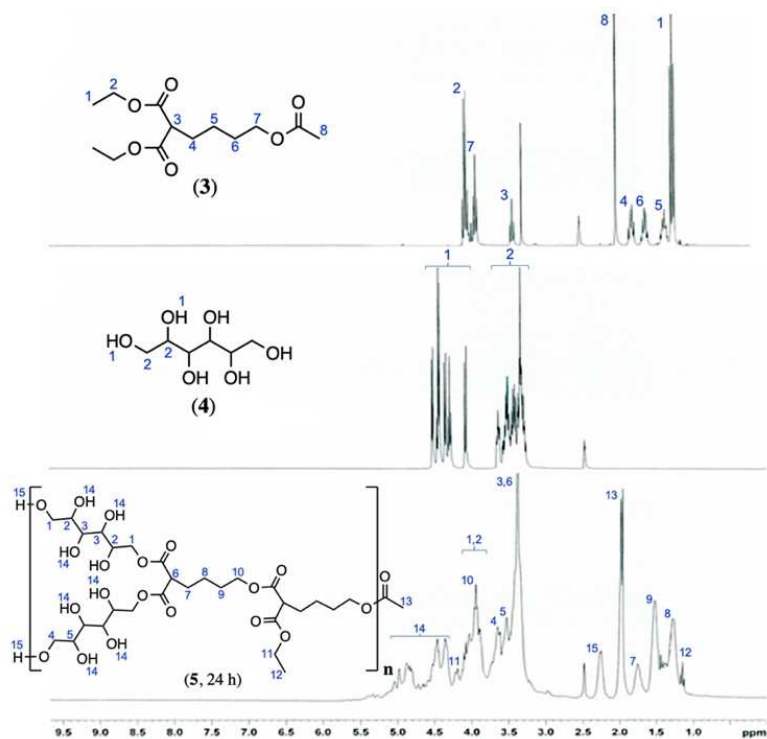
Figure 1. ^{1}H NMR spectra of the monomers (**3, 4**) and the HSPE polymer (**5**, 24 h sample).
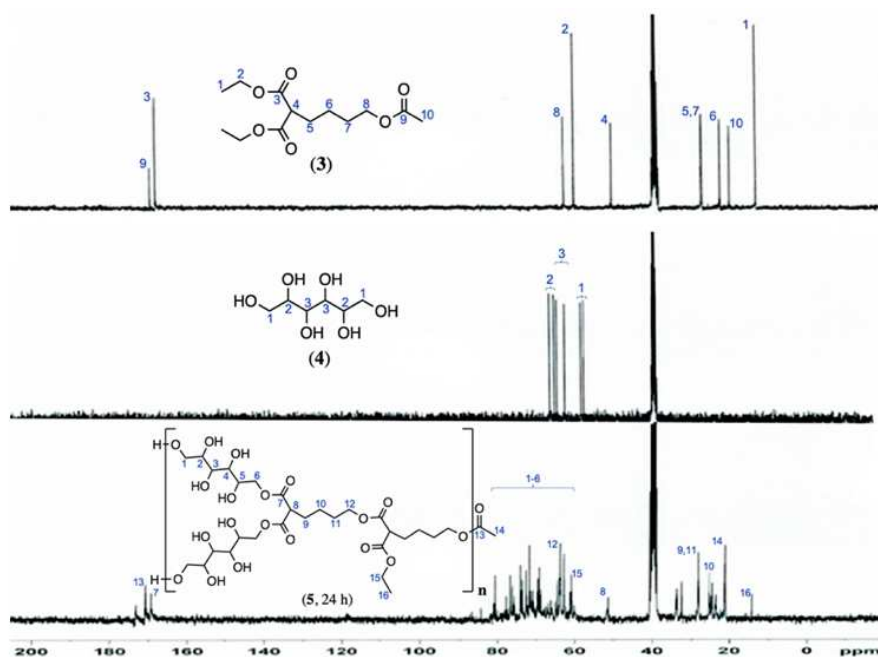

Figure 2. ^{13}C NMR spectra of the monomers (**3, 4**) and the HSPE polymer (**5**, 24 h sample).

with HPLC grade tetrahydrofuran (THF) as the mobile phase (Figure 4B) using a polystyrene standard for calibration. GPC revealed that after reacting for 24 h, we obtained a high molecular weight polymer ($M_w = 36\,150$, PDI$=2.2$). We have seen a regular increase in molecular weight up to 24 h (Figure 4C), however, beyond 24 h of polymerization we noticed a fall in molecular weight, possibly due to crosslinking, which would lead to insoluble polymers (SI, Figure S3).

Successful co-polymerization yielded a three-dimensional polymer (**5**) with amphiphilic cavities and terminal hydroxyl
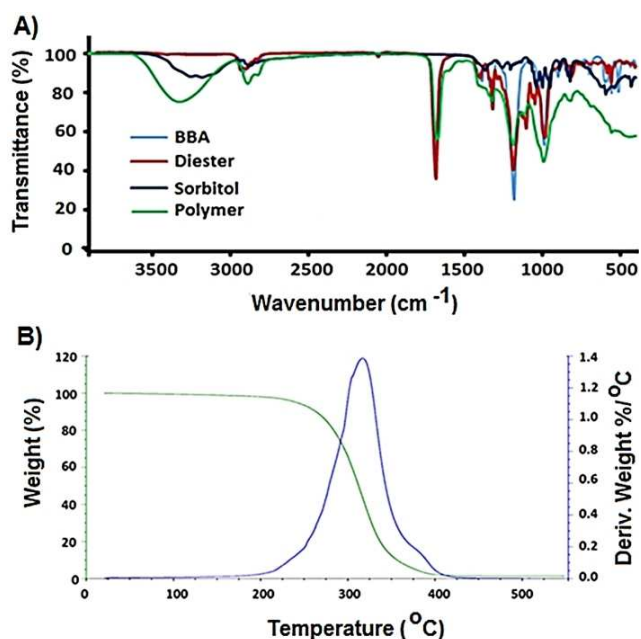
Figure 3. A) FT-IR spectra of the starting material (**2**), the monomers (**3**, **4**), and the HSPE polymer (**5**, 24 h sample). **B**) TGA of HSPE polymer (**5**, 24 h sample).

groups due to the primary and secondary hydroxyl groups on sorbitol. As supported by literature, the synthesized HSPE polymer (**5**) is expected to be biodegradable due to the presence of ester linkages in the polymeric backbone, (Figure 3A).[29–31] When dispersed in aqueous media, the polymer self-assembles with the hydrophobic moieties gathering, bringing out the hydrophilic moieties to interact with the aqueous environment, forming water-dispersed polymeric nanoparticles. Our HSPE polymeric nanoparticle's biodegradability, three-dimensional structure, amphiphilic cavities, functional surface, and stability in water would make it a highly attractive material for the pharmaceutical industry. Further applications of our HSPE polymeric nanoparticles include the field of medicine for the targeted delivery of encapsulated drugs and dyes, achieved by conjugating tumor targeting ligands to the polymer's functional surface groups using water-based carbodiimide chemistry (Scheme 2).

Our HSPE polymer (**5**) was used to synthesize a drug and dye encapsulating HSPE polymeric nanoparticle (**6**), and then further functionalized with folic acid (**7**) to selectively deliver therapeutic molecules to cancer cells. In our first experiment, we have encapsulated a hydrophobic fluorescent dye (Dil dye, 5 μg/μL) and hydrophobic drug (Taxol, 2 μg/μL) in the HSPE
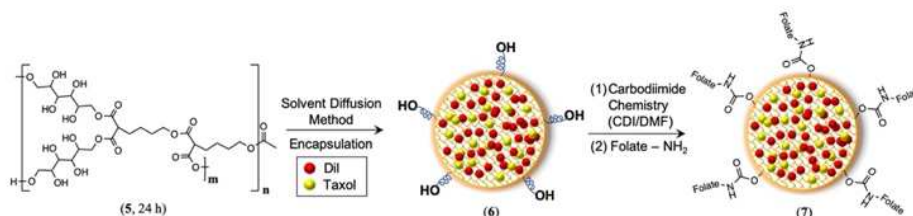
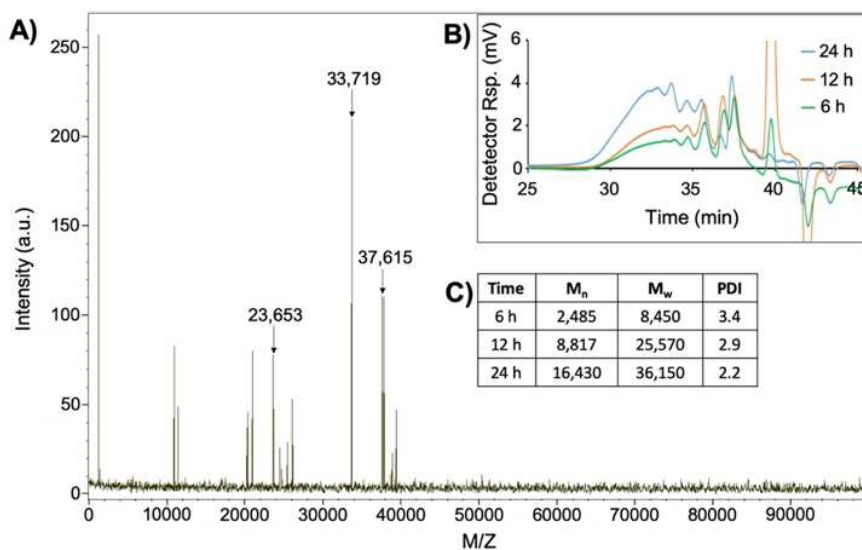**Scheme 2.** Synthesis of functional HSPE polymer-based drug delivery system.

Figure 4. A) MALDI-TOF chromatogram of the 24 h HSPE polymer. **B**) GPC chromatograms of the 6 h, 12 h and 24 h HSPE polymers. **C**) Time dependent progress of polymer formation as monitored by GPC.

polymeric nanoparticles (**6**–**7**, Scheme 2). In short, the HSPE polymer (35 mg), DiI dye (1 µL), and Taxol (5 µL) were dissolved in 250 µL of DMF, mixed and then added dropwise to DI water (4 mL) resulting in the formation of our drug-loaded HSPE polymeric nanoparticles. When dispersed in water, the hydrophobic moieties of the HSPE polymer are forced to gather together and turn inside toward themselves, and the hydrophobic nature of the dye and drug forces them to order themselves within the amphiphilic cavities of the HSPE polymer. At the same time, the polymer's hydrophilic segments are exposed to the aqueous solution and are stabilized through hydrogen bonding between the terminal hydroxyl groups and water. This process results in the formation of hydroxyl-functionalized, therapeutic drug-encapsulating, three-dimensional polymeric nanoparticles (**6**) as an aqueous suspension. It is important to note that our polymeric nanoparticles would also be ideal for the encapsulation and delivery of amphiphilic theranostics as well, due to the amphiphilic nature of the polymeric cavities. Next, we have synthesized aminated folic acid as previously reported[26] (SI, Scheme S2) which we conjugated to the surface of the HSPE nanoparticles. This is easily achieved through water-based carbodiimide chemistry.

To facilitate the internalization of loaded HSPE nanoparticles by prostate-specific membrane antigen (PSMA) positive LNCaP cancer cells, we intend to conjugate folic acid to the surface of the HSPE nanoparticles as a PSMA receptor targeting ligand.[32] For the folate conjugation, CDI (10 mmol) in DMF is mixed and briefly incubated with the drug-dye-loaded HSPE (1 mmol) nanoparticles (**6**). Then, the previously synthesized aminated folic acid (10 mmol) solution is added to the CDI/HSPE-NPs solution and incubated for 3 h at room temperature, then dialyzed (MWCO 6–8 K) against DI water. To characterize the now purified folate-conjugated, drug-dye-loaded HSPE nanoparticles (**7**) were analyzed with Dynamic Light Scattering, ζ-potential, UV-Vis, and fluorescence (Figure 5). DiI and Taxol were successfully encapsulated with high efficiency ($EE_{DiI} = 65\%$, $EE_{Taxol} = 78\%$) as described in the experimental section. The observed higher encapsulation efficiency of our HSPE polymer directly relates to the amphiphilic nature of the polymeric cavities. We stored these HSPE nanoparticle theranostics at 4 °C and determined their stability over time via DLS studies (SI, Table S1).

DLS studies revealed the drug-dye encapsulated HSPE nanoparticles (**6**) had an average hydrodynamic diameter of 88 ± 2 nm (SI, Table S1), and that of folate-conjugated HSPE nanoparticle (**7**) was found to be 93 ± 2 nm (Figure 5A). We characterized the drug-dye-encapsulated HSPE nanoparticles (**6**), and folate-functionalized drug-dye-encapsulated HSPE nanoparticles (**7**) by their surface charge, found by measuring the ζ-potential (Figure 5B). This shift in ζ-potential confirmed the successful conjugation of folic acid to the surface hydroxyl functionality of the HSPE nanoparticles. The long-term stability of these HSPE nanoparticles was investigated by DLS and proved to be very stable in aqueous buffered solution for extended periods without noticeable precipitation or agglomeration (SI, Table S1). The UV-Vis study of the HSPE nanoparticles revealed absorption peaks at 355 and 565 nm, confirming the
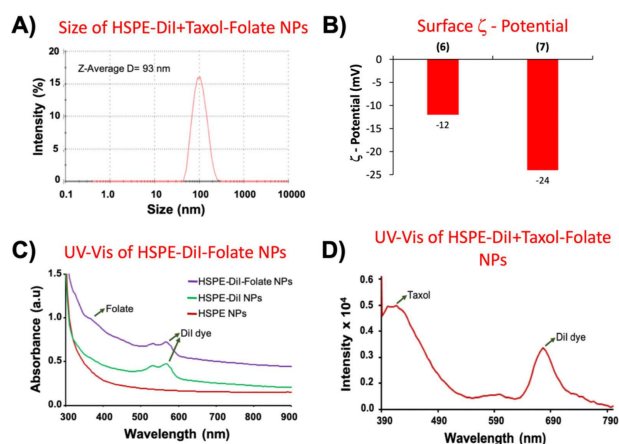
Figure 5. **A**) Dynamic light scattering confirmed the formation of folate-conjugated HSPE nanoparticles with an average diameter of 93 ± 2 nm. **B**) Zeta-potential of cargo-loaded HSPE nanoparticles (**6**) was found to be −12 mV and the Zeta-potential folate-conjugated, cargo-loaded HSPE nanoparticles (**7**) was found to be −24 mV. **C**) UV-Vis study of HSPE nanoparticles confirm the successful conjugation of folic acid ($\lambda_{abs} = 355$ nm) to its surface and the presence DiI dye ($\lambda_{abs} = 565$ nm) within the cavities of the HSPE nanoparticles. **D**) Fluorescence emission spectrum further confirmed the successful encapsulation of Taxol ($\lambda_{em} = 420$ nm) and DiI dye ($\lambda_{em} = 680$ nm).

conjugation of folic acid and encapsulation of DiI dye, respectively (Figure 5C). Fluorescence emission maxima at 420 and 680 nm further confirmed the successful encapsulation of Taxol and DiI dye, respectively (Figure 5D).

We used MTT assays to determine the cytotoxicity of the HSPE nanoparticles where prostate cancer cells (LCNaP) and CHO cells were seeded in 96-well plates and incubated with 1) HSPE nanoparticles, 2) HSPE-DiI-Folate nanoparticles, and 3) HSPE-DiI + Taxol-Folate nanoparticles (**7**) for 24 h. The results (Figure 6) indicated no significant cytotoxicity for both cell lines incubated with unloaded, unconjugated HSPE nanoparticles (OH). Additionally, both cell lines showed similar low cytotoxicity when incubated with folate-conjugated DiI loaded HSPE nanoparticles (FOLATE) due to the lack of the cytotoxic drug, Taxol. This low cytotoxicity also shows that our HSPE nanoparticles are not cytotoxic themselves. However, when incubating both cell lines with the folate-conjugated, drug-dye
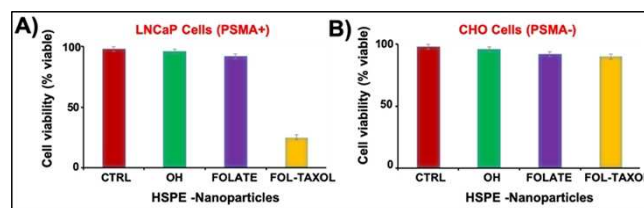
Figure 6. Determination of cytotoxicity of functional HSPE nanoparticles using MTT assay. **A**) The functional HSPE nanoparticles loaded with DiI and Taxol indicated more than 75% LNCaP cell death within 24 h, whereas **B**) no significant cytotoxicity (around 5% cell death) was indicated in CHO cells due to the absence of PSMA receptors that would be expressed on the cell membrane. The minimum toxicity observed from the HSPE nanoparticles (OH) and HSPE-DiI-Folate nanoparticles (FOLATE) is expected due to the lack of the cytotoxic drug. Ctrl: Cells without HSPE nanoparticle treatment.

encapsulated nanoparticles (FOL-TAXOL) (**7**), the LNCaP cell line showed significant cytotoxicity achieving more than 75% cell death (Figure 6A) while the CHO cell line indicated no significant cytotoxicity (5%) (Figure 6B). This difference in cell viability is because CHO cells are PMSA(-), so the folate-conjugated nanoparticles are not internalized, while the LNCaP cancer cell line, being PMSA(+), is selectively targeted. When viewed as a whole, these results support the principle that folate-conjugated HSPE polymeric nanoparticles can target and deliver chemotherapeutics to PMSA(+) cancer cells over healthy cells.

Drug release experiments were conducted to determine how well our HSPE nanoparticle releases Taxol within a tumor microenvironment (low pH) and under conditions of biodegradation (esterase enzyme). This study is important because the rate and level of release of the encapsulated drug will determine the therapeutic efficacy of our HSPE nanoparticles. To determine the time dependent release of Taxol, we used a dynamic dialysis technique at 37 °C (biological temperature). As shown in Figure 7, the results indicated at physiological pH (7.4) there was an initial nominal release (< 10%) of Taxol within the first 12 h and then remained stable for the duration of the study (36 h). This indicated the biostability of our synthesized HSPE polymer under physiological conditions. However, under enzymatic and low-pH conditions (mimicking the tumor microenvironment) HSPE nanoparticles are easily degraded, releasing their encapsulated cargo. As seen, under acidic conditions the polymer backbone is rapidly degraded, releasing 80% of the cargo within 6 hours attributed to the sensitivity of esters to acid hydrolysis. On the other hand, we hypothesize that under esterase conditions the slightly slower release can be attributed to high flexibility of the polymer backbone. Taken together, the results indicate the biodegradability and efficient drug release capability of HSPE nanoparticles for their potential use as a drug delivery system.
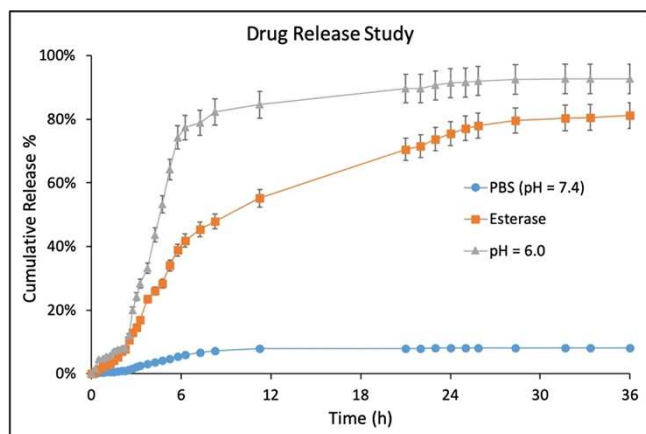
Figure 7. Drug-release profile of HSPE-Taxol-Folate nanoparticles (**7**) using a dynamic dialysis method. The release of Taxol was monitored over time via high performance liquid chromatography (HPLC) in the presence of esterase enzyme (orange square) and in PBS at pH 6.0 (grey triangle). The release of Taxol was minimal (< 10%) under physiological conditions in PBS at pH 7.4. The results are an average of three measurements and were recorded and plotted with ± standard error in terms of % cumulative release.

Internalization studies performed on both the LNCaP and CHO cell lines demonstrate the therapeutic applications of our HSPE nanoparticles. The cell lines (10,000 cells/dish) were treated with various functional HSPE nanoparticles to evaluate the potential biomedical and drug delivery applications for our HSPE nanoparticles. Upon incubation with unconjugated, DiI-loaded HSPE nanoparticles (**6**), the LNCaP cells showed neither internalization nor cell death (Figure 8a–d). However, successful internalization of our folate-conjugated, DiI-loaded HSPE nanoparticles was observed in LNCaP cells without cell death. This internalization is due to the presence of folate on the surface of the nanoparticles (Figures 8 e–h). As hypothesized, we observed successful internalization and cell death in LNCaP cells incubated with HSPE-DiI + Taxol-Folate nanoparticles (**7**) due to surface conjugation with folic acid and the cytotoxic effects of Taxol (Figure 8i–l). Evaluation of our HSPE nanoparticles' cytotoxicity was further evaluated with CHO cells where results indicated no noticeable internalization (Figure 8m–p). This phenomenon is due to the conjugation of our nanoparticles with folate, a ligand having a high affinity to the PSMA receptor which is overexpressed by LNCaP cancer cells; thus, it is possible to target and deliver therapeutic drugs and dyes to tumors while minimizing their toxicity to healthy cells.

Conclusion

In conclusion, a novel hyperstar polyester (HSPE) polymer was synthesized from a diester and bio-based monomer (sorbitol) with amphiphilic cavities and hydrophilic hydroxyl functional groups. The amphiphilic cavities and hydrophilic functional groups played an important role in the successful encapsulation of wide-range of therapeutic drugs and optical dyes. In addition, incorporating sorbitol into the polymer backbone increased the polymer's solubility in organic solvents and allowed for the encapsulation of a wide range of therapeutic molecules. Also, the ability to conjugate the hydroxyl pendants to folate was of a great advantage for the specific targeting of cancer cells without harming healthy cells. The cytotoxicity assessment of the folate-conjugated, drug-dye loaded HSPE nanoparticles revealed high toxicity to the PSMA(+) cancer cells (LNCaP) and minimal toxicity (5%) to the healthy cells (CHO). This is due to the lack of overexpression of the PSMA receptor in the healthy cells. Our HSPE nanoparticles demonstrate great capability for cargo encapsulation and release, minimal toxicity, and surface functional groups that allow the attachment of ligands for targeting specific cells. These attributes make them promising candidates for use as a drug delivery system with the potential to target other cancerous cell lines in vivo, with the ultimate goal of reaching the clinical settings.

Experimental Section

Materials. Dimethylsulfoxide, dimethylformamide, acetonitrile, and diethyl malonate were obtained from Sigma Aldrich and used without any further purification. Near-infrared fluorescent dyes (DiR-D12731 and DiI-D282) and Taxol were purchased from
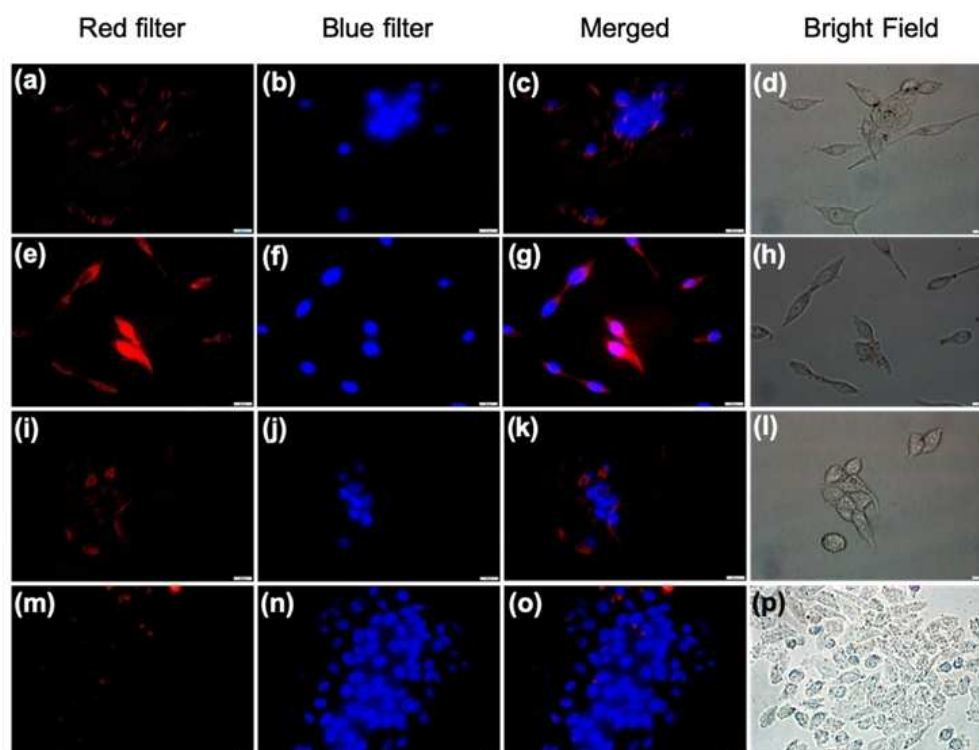
Figure 8. Evaluation of HSPE nanoparticle cellular uptake and cytotoxicity using fluorescence microscopy (scale bar: 500 nm). (**a–d**) Minimal internalization was observed with unconjugated HSPE nanoparticles loaded with DiI dye due to the absence of folate. (**e–h**) Successful internalization was observed with folate-conjugated HSPE nanoparticles loaded with DiI. (**i–l**) LNCaP cells incubated with folate-conjugated nanoparticles loaded with DiI and Taxol showed changes in cellular morphology, which indicated cell death. (**m–p**) CHO cells were incubated with folate-conjugated nanoparticles loaded with DiI and Taxol showed no substantial internalization, as expected.

Invitrogen. Deuterated solvents ($CDCl_3$ and DMSO-d_6), were purchased from Cambridge Isotope Laboratories, Inc. for NMR experiments. 2,5-dihydroxybenzoic acid (DHB) was purchased from Bruker for use as a sample matrix in MALDI-TOF mass spectroscopy. Bio-based monomer (Sorbitol), a catalyst potassium methoxide (KOMe), 3-(4,5-dimethylthiazol-2-yl)-2,5-diphenyltetrazolium bromide (MTT), 4′,6-diamidino-2-phenylindole (DAPI), ethylenediamine (EDA), N-hydroxysuccinimide (NHS), 1-Ethyl-3-[3-dimethylaminopropyl] carbodiimide hydrochloride (EDC), 1,1′-Carbonyldiimidazole (CDI), trifluoroacetic acid (TFA), and regular solvents including tetrahydrofuran, hexane, and ethyl acetate were purchased from Fisher Scientific. The PD-10 columns were purchased from GE Healthcare. Healthy cell, Chinese hamster ovarian (CHO), and prostate cancer LNCaP cells were obtained from American Type Culture Collection (ATCC).

Characterization. Infrared spectra were taken on a PerkinElmer Spectrum TWO FT-IR spectrometer. UV/Vis spectra were recorded using a CARY 100 Bio UV/Vis spectrophotometer. NMR spectra were recorded on Bruker's DPX-300 spectrometer using the TMS/solvent (DMSO-D_6 or $CDCl_3$) signal as an internal reference, and the mass spectroscopy chromatogram was recorded on Bruker's MALDI-TOF MS microflex™ LRF using DHB as the support matrix, and TFA as the ion-pair reagent. Gel permeation chromatography (GPC) results were obtained using a Shimadzu SIL-20 A with a light scattering precision detector. Thermal gravimetric analyses (TGA) results were obtained using TA Instruments's TGA Q50, with sample sizes of around 10 mg. The overall surface charge (ζ potential) and the dynamic light scattering (DLS) studies of the HSPE nanoparticles were obtained using a Zetasizer Nano ZS90 from Malvern Instruments. Analytical Thin Layer Chromatography (TLC) was performed

on aluminum-backed silica gel plates and were visualized in an iodine chamber. Column chromatography was performed using silica gel, and the eluent is mentioned in the procedures below for each case. MTT assay was done using the TECAN Infinite M200 PRO multi-detection microplate reader. Microscopic images were taken using an Olympus IX73 inverted microscope.

Synthesis of hyperstar polyester (HSPE) polymer (5). First, we have synthesized 4-bromobutyl acetate (**2**) and the diester A$_2$B monomer (**3**, Scheme 1) by following a previously reported protocol[21] and as described in the Supporting Information (Supporting Information, Scheme S1). These two monomers (**2**, **3**) were purified and characterized using spectroscopic methods (SI, Figure S1; Figure 1). For the synthesis of HSPE polymer (**5**), the purified monomer (**3**) (1.0 g, 3.647 mmol) and the catalyst, potassium methoxide (100:1 molar ratio), were taken in a 10 mL round bottom flask and heated to 140 °C in a silicone oil bath under medium vacuum for 1 h. The evolution of the by-product (ethyl acetate vapor) was visible after heating the sample. Subsequently, sorbitol (1.324 g, 7.288 mmol) was added and continued heating under a nitrogen atmosphere for the next 12 h. Next, high vacuum (4×10^{-4} mm/Hg) was applied to the reaction mixture for the desired hours of reaction (11–35 h), maintaining the same reaction conditions. The resulting polymer was purified using the solvent precipitation method. In this case, a concentrated solution of the polymer in DMF was prepared and precipitated in acetone.

Yield: (78%). ^{1}H NMR (300 MHz, DMSO-d_6, δ ppm). 1.29 (m, 3H), 154 (m, 2H), 1.76 (m, 2H), 1.75 (m, 2H), 1.99 (m, 2H), 2.37 (m, 2H), 3.34 (m, 2H), 3.52 (m, 2H), 3.66 (m, 2H), 3.96 (m, 2H), 4.35(m, 2H), 4.49 (m, 2H), 3.87 (m, 2H). ^{13}C NMR (75 MHz, DMSO-d_6, δ ppm): 21.12,

28.32, 51.44, 60.88, 62.73, 64.08, 71.79, 72.63, 74.30, 79.8, 170.91. FT-IR: 3405, 2944, 1724, 1372, 1236, 1040 cm^{-1}. TGA: 10% weight loss was detected at 265 °C.

Synthesis of DiI and Taxol co-encapsulating HSPE nanoparticles (6). First, we made a polymer solution by dissolving 35 mg of HSPE polymer into 250 μL of DMF. Then the optical dye DiI (1 μL, 5 μg/μL) and cytotoxic drug Taxol (5 μL, 2 μg/μL) were mixed into 250 μL of DMF. The drug/dye and polymer solutions were then combined and vortexed for 10 minutes, followed by mixing on a table mixer for 15 minutes. The resulting polymer-cargo solution was added drop-wise (10 seconds between each) to 4 mL of DI water with continuous stirring at room temperature. The synthesized nanoparticles were purified against a PD-10 column (GE Healthcare) and dialyzed (MWCO 6–8 K) against PBS (pH = 7.4).

Synthesis of folate-functionalized, DiI and Taxol co-encapsulating HSPE nanoparticles (7). First, we synthesized aminated folic acid by following our previously reported method[26] which is described briefly in the Supporting Information (Scheme S2). The folate-functionalized HSPE nanoparticles were made by conjugating the synthesized aminated folic acid with our hydroxylated HSPE nanoparticles using CDI chemistry. First, CDI (10 mmol) was dissolved in 100 μL of DMF and then added dropwise to the DiI/Taxol co-encapsulating HSPE nanoparticle solution (6, 1 mmol) and incubated for 15 minutes on the table mixer. The aminated folic acid solution (10 mmol) was then added and incubated for 3 h on the table mixer at room temperature. The newly formed folate-functionalized, cargo-loaded HSPE nanoparticles (7) were dialyzed (MWCO = 6–8 K) against DI water for 24 h. The encapsulation efficiency of our HSPE nanoparticles was measured using UV-Vis spectroscopy and the following equation, EE% = [(Cargo added − Free cargo)/Cargo added] × 100. The concentration of taxol drug was found to be 0.22 μg/ mg of HSPE nanoparticle. The resulting HSPE nanoparticles (7, 2.7 mmol) were stored at 4 °C, ready for cancer targeting and treatment experiments when needed.

Cell Cultures. Human prostate cancer cells (LNCaP) and noncancerous Chinese hamster ovarian cells (CHO) were obtained from ATCC and maintained according to the provider's protocols. In short, we grew the LNCaP cells in 89% DMEM medium, and we grew the CHO cells in Kaighn's modification of Ham's F12K medium, both supplemented with 10% heat-inactivated FBS and 1% penicillin-streptomycin, by volume. We maintained the cell lines at 37 °C under a 5% CO$_2$ atmosphere in a humidified incubator.

MTT Assay. We began the assay 24 h after the LNCaP and CHO cells were added to their respective 96-well microplate (2,500 cells/well). After this period, the cells were incubated with different HSPE nanoparticles (25 μL, 2.7 mmol) for 24 h at 37 °C. Following the incubation period, the cells were washed three times with 1X PBS, then treated with 30 μL of MTT (5 μg/μL) solution and incubated for 2 h. At this point we observed the formation of formazan crystals which we dissolved with acidified isopropanol (0.1 N HCl) for absorbance readings. We recorded the formazan absorbance in each well at 570 nm and 750 nm (background) using the Infinite M200 PRO microplate reader (Figure 6). These readings determined the concentration of formazan in each well and revealed the cell viability for each HSPE nanoparticle tested. We experimented with groups of three for each series.

In Vitro Drug Release. The *in vitro* drug release studies were performed using a dynamic dialysis technique at biological temperature (37 °C). In this technique, 100 μL of HSPE nanoparticles (7) were incubated with 20 μL of porcine liver esterase in a dialysis bag (MWCO 6–8k) and placed in a solution of PBS at pH 7.4. The amount of drug released to the outer reservoir from the nanoparticle was determined at regular time intervals using HPLC. The amount of released drug was calculated against a standard calibration curve and the cumulative release (%) was calculated using:

$$\text{cumulative release } (\%) = [\text{drug}]_t / [\text{drug}]_0 \times 100$$

where $[\text{drug}]_t$ = amount of drug released at time t, and $[\text{drug}]_0$ is the amount of drug encapsulated within the HSPE nanoparticles.

Fluorescence Microscopy. Both the LNCaP and CHO cell lines were grown on cell culture dishes 24 h before treatment with HSPE nanoparticles. After a 24 h incubation period with the HSPE nanoparticles, the cells were stained with DAPI dye, washed twice with 1X PBS, and then fixed with 4% paraformaldehyde. Using an inverted fluorescence microscope (Olympus IX73), both the experimentally treated and controls dishes of both cell lines were analyzed to observe the internalization of our HSPE nanoparticles, visualized by the DAPI (blue) and DiI (red) dyes (Figure 8).

Acknowledgements

Conflict of Interest

The authors declare no conflict of interest.

[1] D. Shenoy, S. Little, R. Langer, M. Amiji, *Mol. Pharm.* **2005**, *2*, 357–366.
[2] K. S. Soppimath, T. M. Aminabhavi, A. R. Kulkarni, W. E. Rudzinski, *J. Controlled Release* **2001**, *70*, 1–20.
[3] R. Chandra, *Prog. Polym. Sci.* **1998**, *23*, 1273–1335.
[4] L. S. Nair, C. T. Laurencin, *Prog. Polym. Sci.* **2007**, *32*, 762–798.
[5] B. D. Ulery, L. S. Nair, C. T. Laurencin, *J. Polym. Sci. Part B* **2011**, *49*, 832–864.
[6] H. Tian, Z. Tang, X. Zhuang, X. Chen, X. Jing, *Prog. Polym. Sci.* **2012**, *37*, 237–280.
[7] C. G. Pitt, T. A. Marks, A. Schindler, *NIDA Res. Monogr.* **1981**, *28*, 232–253.
[8] S. Li, M. Vert in *Degradable Polymers,* (Eds.: G. Scott), Springer, Dordrecht, **2002**, pp. 71–131.
[9] I. Vroman, L. Tighzert, *Materials* **2009**, *2*, 307–344
[10] S. Hindi, M. Albureikan, S. Al-Sharabi, *J. Nanosci. Nanotechnol.* **2017**, *4*, 49–58.
[11] E. R. Gillies, J. M. J. Fréchet, *Drug Discovery Today* **2005**, *10*, 35–43.
[12] L. Y. Qiu, Y. H. Bae, *Pharm. Res.* **2006**, *23*, 1–30.
[13] Y. Wang, S. M. Grayson, *Adv. Drug Delivery Rev.* **2012**, *64*, 852–865.
[14] F. Zhang, M. Elsabahy, S. Zhang, L. Y. Lin, J. Zou, K. L. Wooley, *Nanoscale* **2013**, *5*, 3220–3225.
[15] F. Zhang, S. Zhang, S. F. Pollack, R. Li, A. M. Gonzalez, J. Fan, J. Zou, S. E. Leininger, A. Pavía-Sanders, R. Johnson, *J. Am. Chem. Soc.* **2015**, *137*, 2056–2066.
[16] D. A. Tomalia, H. Baker, J. Dewald, M. Hall, G. Kallos, S. Martin, J. Roeck, J. Ryder, P. Smith, *Macromolecules* **1986**, *19*, 2466–2468.
[17] P. R. Ashton, D. W. Anderson, C. L. Brown, A. N. Shipway, J. F. Stoddart, M. S. Tolley, *Chem. Eur. J.* **1998**, *4*, 781–795.
[18] J. M. J. Fréchet, D. A. Tomalia in *Dendrimers and Other Dendritic Polymers, Vol. 1* (Eds.: J. M. J. Fréchet, D. A. Tomalia), Wiley & Sons, Chichester, **2002**, pp. 1–44.
[19] C. Gao, Y. Xu, D. Yan, W. Chen, *Biomacromolecules* **2003**, *4*, 704–712.

[20] Y. Zhou, W. Huang, J. Liu, X. Zhu, D. Yan, *Adv. Mater.* **2010**, *22*, 4567–4590.

[21] S. Santra, C. Kaittanis, J. M. Perez, *Langmuir* **2010**, *26*, 5364–5373.

[22] T. Zhang, B. A. Howell, D. Zhang, B. Zhu, P. B. Smith, *Polym. Adv. Technol.* **2018**, *29*, 2352–2363.

[23] J. F. Stumbé, B. Bruchmann, *Macromol. Rapid Commun.* **2004**, *25*, 921–924.

[24] M. Adeli, B. Rasoulian, F. Saadatmehr, F. Zabihi, *J. Appl. Polym. Sci.* **2013**, *129*, 3665–3671.

[25] S. Santra, A. Kumar, *Chem. Commun.* **2004**, *18*, 2126–2127.

[26] S. Santra, C. Kaittanis, J. M. Perez, *Mol. Pharm.* **2010**, *7*, 1209–1222.

[27] S. D. Li, J. D. He, P. H. Yu, M. K. Cheung, *J. Appl. Polym. Sci.* **2003**, *89*, 1530–1536.

[28] W. A. Herrera-Kao, M. I. Loía-Bastarrachea, Y. Pérez-Padilla, J. V. Cauich-Rodríguez, H. Vázquez-Torres, J. M. Cervantes-Uc, *Polym. Bull.* **2018**, *75*, 4191–4205.

[29] C. C. Lee, J. A. MacKay, J. M. J. Fréchet, F. C. Szoka, *Nat. Biotechnol.* **2005**, *23*, 1517–1526.

[30] S. Kaihara, S. Matsumura, A. G. Mikos, J. P. Fisher, *Nat. Protoc.* **2007**, *2*, 2767–2771.

[31] M. Hu, M. Chen, G. Li, Y. Pang, D. Wang, J. Wu, F. Qiu, X. Zhu, J. Sun, *Biomacromolecules* **2012**, *13*, 3552–3561.

[32] S. S. Chang, *Nat. Rev. Urol.* **2004**, *6*, S13–S18.